Available online at www.sciencedirect.com
ScienceDirect
Journal of Photochemistry and Photobiology A: Chemistry 196 (2008) 10–23
Journal of Photochemistry and Photobiology A:Chemistry
www.elsevier.com/locate/jphotochem

Environment sensitive phenothiazine dyes strongly fluorescence in protic solvents ☆

Feng Han [a], Lina Chi [a], Wenting Wu [a], Xiaofen Liang [a], Meiyan Fu [a,b], Jianzhang Zhao [a,*]

[a] *State Key Laboratory of Fine Chemicals, Dalian University of Technology, 158 Zhongshan Road, Dalian 116012, PR China*
[b] *Virtual Laboratory of Computational Chemistry, CNIC, Chinese Academy of Sciences, Beijing, PR China*

Received 27 July 2007; received in revised form 13 October 2007; accepted 12 November 2007
Available online 19 November 2007

Abstract

1,10-Fused ring phenothiazines were found to be a new kind of fluorescent dyes that strongly fluorescence in protic solvents than in aprotic solvents, with higher fluorescence quantum yields (Φ) and longer emission wavelength than the previously reported dyes that with similar solvent sensitivity profile. For example, compound **5** shows a Φ-value of 0.075 in diethyl ether and 0.517 in methanol. Interestingly, a transition from C=C double bond (**5**) to C–C single bond (**4**) in the fused ring switch the photophysical properties completely, i.e. the analogue compound **4** demonstrates the opposite sensitivity, for which $\Phi = 0.099$ in diethyl ether but the fluorescence is quenched completely in methanol. Further derivatization of **5** is convenient, demonstrated by the preparation of compound **6**, for which the unique solvent sensitivity is reserved and higher Φ in protic solvents was observed ($\Phi = 0.739$ in methanol). The solvatochromism of the compounds were analysed with Lippert–Mataga correlation, $E_T^N(30)$ values and multilinear regressions with Catalán and Kamlet–Taft solvents scales. The aprotic and protic solvents appeared as two isolated domains in the Lippert–Mataga plots, whereas fitting with $E_T^N(30)$ scales gives a linear regression comprising both aprotic and protic solvents. Kamlet–Taft scales are more appropriate than the Catalán solvent scales for describing the solvatofluorochromism of the compounds. An intermolecular hydrogen bonding mechanism is proposed for the observed switching of the fluorescence with protic solvents.

Keywords: Fluorescent polarity probes; Phenothiazines; Multilinear regression; Solvatochromism; Solvent sensitivity

1. Introduction

Environment sensitive fluorophores and fluorescent polarity probes, such as the well-known 6-propionyl-2-(dimethylamino) naphthalene (PRODAN), 1-anilinonaphthalene-8-sulfonic acid (ANS), have been widely used in the study of molecular recognition (as chemosensors), proteins or membrane structures and interactions, etc. [1–10]. Normally a fluorescent probe is weakly fluorescent in hydrophilic environment (or in more polar solvents) but strongly fluorescent in hydrophobic environment. Fluorophores with the opposite sensitivity profile, i.e. the dyes which strongly fluorescence in protic solvents whereas show weak fluorescence in aprotic solvents, also attracted much attention [11]. However, only few fluorophores are entitled with this unique property, such as acridine [12], pyrene-3-carboxaldehyde (**1**) and 7-methoxy-4-methylcoumarins (**2**), etc. (Scheme 1) [13,14].

Very recently, a new fluorescent dye **3** (Scheme 1) was reported as strongly fluorescent dye in protic solvents with longer emission wavelength, but weakly fluorescent in aprotic solvents, with $\Phi = 0.0003$ and 0.21 in hexane and methanol ($\lambda_{em} = 469$ nm), respectively [11]. However, new fluorophores are desired, especially in the aspects of longer emission wavelength, higher quantum yields and easy derivatization [11–14].

Herein we report 1,10-fused ring phenothiazine dyes as a new kind of solvent sensitive fluorescent dyes with the unique sensitivity of strongly fluorescence in protic solvents than in aprotic solvents, such as **5** (Scheme 1), with higher quantum yields and longer emission wavelength than the reported dyes. Further derivatization of this structure profile is easy, as demon-

☆ Supplementary data associated with this article can be found, in the online version, at: doi:10.1016/j.jphotochem.2007.11.007.

* Corresponding author. Tel.: +86 411 3960 8007; fax: +86 411 3960 8007.
E-mail address: zhaojzh@dlut.edu.cn (J. Zhao).

1010-6030/$ – see front matter © 2007 Elsevier B.V. All rights reserved.
doi:10.1016/j.jphotochem.2007.11.007

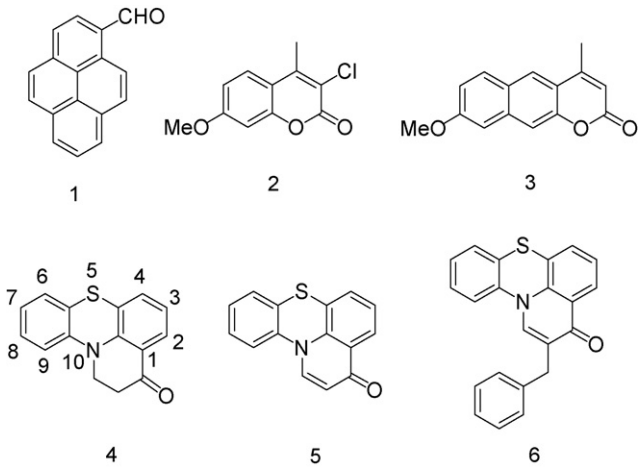

Scheme 1. Environment sensitive fluorescent dyes.

strated by preparation of compound **6**, for which even higher quantum yield was observed.

Interestingly, complete switching effect of the photophysical properties was found for **4**, which is a close analogue of compound **5**. Compound **4** is fluorescent in aprotic solvents, whereas the emission is completely quenched in protic solvents such as methanol.

To study the solvatochromism/solvatofluorochromism of these 1,10-fused ring phenothiazine derivatives, UV–vis absorption and fluorescence spectroscopic data were collected. The solvatochromism of compounds **4–6** were analysed with Lippert–Mataga correlation [4,5], solvent scales of normalized molar electronic transition energies, i.e. the $E_T^N(30)$ values [15], and multilinear regression with the Catalán [16–19] and Kamlet–Taft solvent scales [20]. Solvent-dependent fluorescence intensity and lifetimes were also studied. The fluorescence intensity of **5** in aqueous MeOH solution was found to be pH-independent in the range of pH 4.0–11.0.

2. Experiments

2.1. General procedures and materials

All the chemicals for the synthesis or the solvents for spectrum measurement are analytical or spectroscopic grade and were used as received without further purification. NMR spectra were recorded on a Varian INOVA spectrometer (400 MHz for ^{1}H). UV–vis absorption spectra were recorded on a PerkinElmer Lambda 35 UV–vis spectrophotometer. Fluorescence spectra were recorded with JASCO FP-6500 spectrometer and Sanco 970CRT fluorospectrometer. The fluorescence lifetime was measured with frequency-domain instrument of Chronos 95145 fluorescence lifetime spectrometer (ISS, Inc., Champaign, IL, USA). The regression of the experimental curves was carried out with the software VINCI Analysis (BETA 1.6). The UV–vis absorption and fluorescence emission spectra were recorded with non-degassed solutions. The quantum yields were determined with quinine sulfate as the standard ($\Phi = 0.546$, $\lambda_{ex} = 350$ nm).

For the binary solvents (the mixed solvents), the ε_{mix} and the n_{mix} values were estimated from Eqs. (1a) and (1b) [21]. Where the subscripts a and b represent the two different neat solvents and f is the volume fraction of each solvents. The orientation polarizability Δf is varied by increasing the contents of the MeOH in the mixtures and is estimated with Lippert equation (Eq. (3b)).

$$\varepsilon_{mix} = f_a\varepsilon_a + f_b\varepsilon_b \quad (1a)$$

$$n_{mix}^2 = f_a n_a^2 + f_b n_b^2 \quad (1b)$$

All the curves was plotted with Origin 5.0 (Microcal software) or Sigmaplot 2000 (SPSS Inc.). The multilinear regression with the Catalán or the Kamlet–Taft solvent scales was performed with equations implemented within SigmaPlot 2000 (SPSS Inc.). In most case r^2 was used to evaluate the regression quality, although the r values will give apparently a "better" result. Theoretical calculations were carried out with the Gaussian03 program package by using density functional theory (DFT) [22]. All the ground-state molecular structures were optimized on Becke 3-Lee-Yang-Parr (B3LYP) along with 6-31G+(d) basis set to locate the minimum potential energy.

2.2. Synthesis procedures

2.2.1. 2,3-Dihydro-3-keto-lH-pyrido[3,2,l-kl]phenothiazine (4) [23–26]

To the suspension of 20.0 g of phenothiazine (0.1 mol) in 30 mL of acrylonitrile in a 250 mL beaker was added 1 mL of benzyltrimethylammonium hydroxide (38%). A vigorous reaction was initiated after about 20 s and light yellow solid begin to precipitate. The hot reaction mixture was transferred into a flask and was refluxed with stirring for 3 h. After cooling, the yellow solid was collected with suction and was recrystalized from acetone to give 10-(2-cyanoethyl)phenothiazine as yellow solid. 4.44 g, yield: 17.6%. mp 143–144 °C. ^{1}H NMR (400 MHz, $CDCl_3$, 25 °C, TMS) δ 2.79 (t, 2H, $J = 7.2$ Hz), δ 4.20 (t, 2 H, $J = 7.2$ Hz), 6.80–6.82 (m, 2 H), 6.94–6.97 (m, 2H), 7.15–7.19 (m, 4H). ^{13}C NMR (100 MHz, $CDCl_3$, 25 °C, TMS) δ 144.0, 128.0, 127.6, 126.3, 123.6, 117.7, 115.4, 43.5, 16.6. LRMS (ESI): found, 253.1 (100, calcd for $[M+1]$, 253.1). Element analysis calcd for $C_{15}H_{12}N_2S$: C 71.40, H 4.79 and N 11.10, found C 71.38, H 4.74 and N 10.84.

A mixture of 10-(2-cyanoethyl)phenothiazine (10.0 g, 3.96 mmol), NaOH (11.0 g, 275 mmol) in solvent of methanol/water (110 mL/30 mL) was heated to reflux and stirred for 15 h until all the solid dissolved. Then the mixture was poured into mixture of ice/water, the insoluble solid was removed by filtration and the filtrate was acidified with concentrated HCl, pale white solid appeared and was collected with suction, recrystalized from 80% ethanol. 10-(2-Carboxyethyl)phenothiazine was obtained as colorless needles, 4.40 g, 50.0%. mp 155–156 °C. ^{1}H NMR (400 MHz, $CDCl_3$, 25 °C, TMS) δ 2.86 (t, 2H, $J = 8.0$ Hz), δ 4.19 (t, 2H, $J = 8.0$ Hz), 6.86–6.94 (m, 4H), 7.15–7.19 (m, 4H). LRMS (ESI-negative): found, 270.0 (5, calcd for $[M-1]$, 270.1), 306.0 (100, calcd for $[M+Cl]$, 306.0), 308.0 (35, calcd for $[M+Cl]$, 308.0), 541.1

(80, calcd for [2*M* − H], 541.1). Element analysis calcd for $C_{15}H_{13}NO_2S$: C 66.40, H 4.83 and N 5.16, found C 66.40, H 4.79 and N 5.09.

A mixture of 10-(2-carboxyethyl)phenothiazine (4.4 g, 16.2 mmol), 20 mL of dry benzene and 3.5 g (16.37 mmol) of trifluoroacetic anhydride was heated to reflux and stirred for 1 h. The reaction mixture was poured into cracked ice. The benzene solution was washed with aqueous sodium carbonate to remove the starting material. The benzene layer was dried over anhydrous sodium sulfate and evaporated to dryness. The resulting yellow solid was purified by column chromatography with dichloromethane (DCM) as eluent (silica gel, $R_f = 0.59$). 2.73 g yellow solid of **4** was obtained, yield: 66.5%. mp 105–106 °C. ^{1}H NMR (400 MHz, $CDCl_3$, 25 °C, TMS) δ 2.87 (t, 2H, $J = 8.0$ Hz), δ 4.08 (t, 2H, $J = 8.0$ Hz), 6.90–7.00 (m, 3H), 7.13–7.26 (m, 3H), 7.70 (d, 1H, $J = 8.0$ Hz). ^{13}C NMR (100 MHz, $CDCl_3$, 25 °C, TMS) δ 192.9, 147.3, 142.9, 132.3, 128.0, 127.7, 125.9, 123.6, 122.5, 122.3, 122.2, 121.5, 114.0, 44.4, 36.4; LRMS (ESI): found, 252.1 (100, calcd for [*M* + H], 254.1). Element analysis calcd for $C_{15}H_{11}NOS$: C 71.12, H 4.38 and N 5.53, found C 71.05, H 4.33 and N 5.45. It is proposed that **4** is liable to form **5** under the condition of the MS spectral measurement. This is also observed on the TLC plate. Initially the dot of **4** is dark yellow fluorescent under UV light, soon after it shows the characteristic fluorescence of **5**.

2.2.2. 3-Keto-1H-pyrido[3,2,l-kl]phenothiazine (5) [26]

A solution of 0.3 g (1.2 mmol) of **4** in 10 mL of hot carbon tetrachloride was cooled to 50 °C and 5 mL carbon tetrachloride solution containing 1.15 g (7.40 mmol) of bromine was added in several portions. The mixture was heated for 30 min, and the solvent was evaporated to gave a dark red tar. The crude product was purified by column chromatography (silica gel, DCM, $R_f = 0.44$). 0.187 g of 2-bromo-3-keto-2,3-dihyro-1*H*-pyrido[3,2,1-*kl*]phenothiazine was obtained, yield: 47%. mp 74–77 °C (softened, decomposed). ^{1}H NMR (400 MHz, $CDCl_3$, 25 °C, TMS) δ 4.32–4.37 (dd, 1H, $J = 4.0$ Hz), 4.46–4.51 (dd, 1H, $J = 4.0$ Hz), 4.72–7.75 (q, 1H, $J = 4.0$ Hz), 6.96–7.01 (m, 2H), 7.09–7.12 (m, 2H), 7.18–7.26 (m, 2H), 7.76 (d, 1H, $J = 8.0$ Hz).

A mixture of 2-bromo-3-keto-2,3-dihyro-1*H*-pyrido[3,2,1-*kl*]phenothiazine (138 mg, 0.42 mmol), 126 mg sodium acetate (1.54 mmol) and 6 mL glacial acetic acid was stirred at 30 °C for 10 min, the resulted solution was stirred at 60 °C for 12 h. The solvent was evaporated to dryness and the residue was taken up with DCM, washed with brine twice, the organic layer with dried over anhydrous sodium sulfate, after removal of the solvent, the residue was purified with column chromatography (silica gel, DCM/MeOH gradient. $R_f = 0.45$, DCM:MeOH = 10:1). 30 mg of yellow solid was obtained, yield: 28.4%. mp 188–189 °C. ^{1}H NMR (400 MHz, $CDCl_3$, 25 °C, TMS) δ 6.48 (d, 1H, $J = 8.0$ Hz), 7.14 (d, 1H, $J = 8.0$ Hz), 7.22 (d, 1H, $J = 8.0$ Hz), 7.27–7.34 (m, 3H), 7.40 (d, 1H, $J = 8.0$ Hz), 8.04 (d, 1H, $J = 8.0$ Hz), 8.10 (d, 1H, $J = 8.0$ Hz); ^{13}C NMR (100 MHz, $CDCl_3$, 25 °C, TMS) δ 178.5, 139.7, 137.5, 137.0, 128.7, 128.6, 128.0, 127.4, 126.8, 125.9, 124.6, 124.3, 122.1, 119.3, 113.3. LRMS (ESI): found, 251.1 (10, calcd for [*M* + H], 252.0), 274.0 (20, calcd for [*M* + Na], 275.0), 525.0 (10, calcd for [2*M* + Na], 526.1). Element analysis calcd for $C_{15}H_9NOS{\cdot}0.14CH_3OH$: C 71.08, H 3.77 and N 5.47, found C 71.07, H 3.85 and N 5.89.

5 can be directly separated from the bromination step, but with a much lower yield of 3.6%.

2.2.3. 2-Benzyl-3H-pyrido[3,2,1-kl]phenothiazin-3-one (6) [27]

0.38 g of 2,3-dihydro-3-keto-l*H*-pyrido[3,2,l-*kl*]phenothiazine **4** and 0.38 g of benzaldehyde was dissolved in 10 mL ethanol, 0.25 mL of 5 N NaOH was added and the mixture was stirred for 30 min at RT. Dark-red solid precipitate and the solid was collected with suction, mixed with ethanol and refluxed for 2 min in the presence of KOH. The reaction was quenched by addition of water and extracted with DCM. The crude product was purified by column chromatography (silica gel, gradient DCM/MeOH). Yield: 11.7%. mp 155–157 °C. ^{1}H NMR (400 MHz, $CDCl_3$, 25 °C, TMS) δ 8.11 (d, 1H, $J = 8.0$ Hz), 7.67 (s, 1H), 7.33–7.34 (m, 5H), 7.11–7.29 (m, 4H), 7.13–7.15 (d, 1H, $J = 8.0$ Hz), 6.85–6.87 (d, 1H, $J = 8.0$ Hz), 3.99 (s, 2H); ^{13}C NMR (100 MHz, $CDCl_3$, 25 °C, TMS) δ 177.7, 139.6, 139.3, 137.2, 135.8, 129.3, 128.9, 128.5, 128.4, 127.9, 126.6, 126.5, 126.1, 125.7, 125.5, 124.3, 121.7, 119.1, 33.8. LRMS (ESI): found, 342.0 (100, calcd for [*M* + H], 342.1). Element analysis calcd for $C_{22}H_{15}NOS{\cdot}0.25CH_3CH_2OH$: C 76.57, H 4.71 and N 3.98 and found C 76.52, H 4.72 and N 3.81.

3. Results and discussion

3.1. Synthesis

1,10-Fused ring phenothiazines **4**–**6** were prepared according to the literature method (Scheme 2). The purity of the compounds after recrystalization, the only purification method used in literatures [23–28], was found to be not high enough so column chromatography were usually carried out for the purification. The compounds reported in the previous literatures, mainly for synthesis purpose, were devoid of structure elucidating data, such as NMR and mass spectrum [23–28]. Herein full characterization was carried out (for the single crystal structure, see supplementary data).

3.2. Spectroscopic properties

3,7-Substituted phenothiazine derivatives have been thoroughly studied in literatures [29–32], for example, as electroluminescent materials, etc. For the 1,10-fused ring phenothiazine derivatives, however, no photophysical property study has been carried out.

The normalized UV–vis absorption of **4** and **5** are shown in Fig. 1. The main absorption bands (S0–S1 transition) show minor solvent-dependent shifts, indicating only a modest solvatochromism at the ground-state. The absorption of **4** is bathochromically shifted compared to **5**, despite of apparent larger π-electron delocalization in **5**.

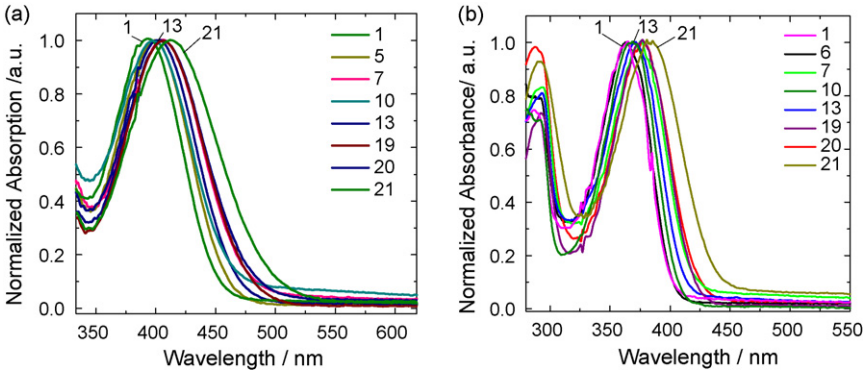

Fig. 1. Selected normalized absorption spectra of **4** (a) ($c = 1.05 \times 10^{-5}$ M) and **5** (b) ($c = 4.06 \times 10^{-6}$ M) in several solvents. The solvents numbers refer to the solvents in Tables 1 and 2.

Different from UV–vis absorption spectra, fluorescence emission of **4** and **5** are strongly solvent dependent, in aspects of both wavelength and intensity (Fig. 2). The more red-shifted emission in polar solvents indicated a more significant charge transfer nature of the emission state due to the solvent effect. The shoulder emission of **4** and **5** in some solvents may be due to the charge transfer state that can undergo structural relaxation leading to different emitting conformation which depend on the solvent characteristics. The photophysical data of **4**–**6** are summarized in Tables 1–3, respectively.

The emission wavelength, fluorescence intensity, fluorescence quantum yields and lifetimes are strongly structure-related and solvent-dependent. For example, compound **4** is fluorescent in aprotic solvents such as THF, DCM, etc., but non-fluorescent in protic solvents, such as in methanol and water ($\Phi < 0.0001$ in MeOH and water, vs. $\Phi = 0.062$ in MeCN and $\Phi = 0.119$ in benzene). This property is similar to the normal polarity probes [4,33], such as PRODAN [1,4,5,10].

On the contrary, **5** is more fluorescent in polar solvents and especially in protic solvents such as methanol and water, than in aprotic solvents ($\Phi = 0.517$ in MeOH, vs. $\Phi = 0.075$ in Et_2O). This profile agrees well with a recently reported fluorescent probe which shows the same reversed polarity sensitivity [11]. Similar to **5**, compound **6** is more fluorescent in protic solvents than in aprotic solvents. Interestingly, higher quantum yield was found for **6** in protic solvents ($\Phi = 0.739$ in MeOH).

Compared to the reported fluorophores with similar polarity sensitivity profile, such as the pyrenecarboxaldehyde ($\Phi = 0.15$ in MeOH) [5,13], or a benzochromen fluorophore **3** reported recently ($\Phi = 0.21$ in MeOH) [11], compound **5** shows higher fluorescence quantum yields (e.g. $\Phi = 0.517$ in MeOH) as well as longer emission wavelength (about 490 nm, vs. 470 nm of the recently reported dye **3**) in MeOH. The quantum yield of **5** is low in acetic acid, possibly due to the protonation of the nitrogen atom.

The fluorescence lifetimes (τ) of **4** remain almost constant in neat aprotic solvents (range from 3.48 ns to 4.82 ns). For **5**, shorter lifetimes of 0.64–1.96 ns were observed. The lifetimes of **5** increase from less than 2 ns in aprotic solvents to 6.3–13.4 ns in protic solvents, correspondingly the fluorescence quantum yields increase dramatically. The fluorescence of **4** is completely quenched in protic solvents.

As the emission of **4** and **5** are strongly solvent dependent, in aspects of emission intensity and wavelength, thus, the visual effect of the polarity dependency of the fluorescence of **4** and **5** was examined (Fig. 3). It can be seen clearly that with increasing of the solvent polarity, especially switching from aprotic to protic solvents, **4** and **5** demonstrated exactly opposite response,

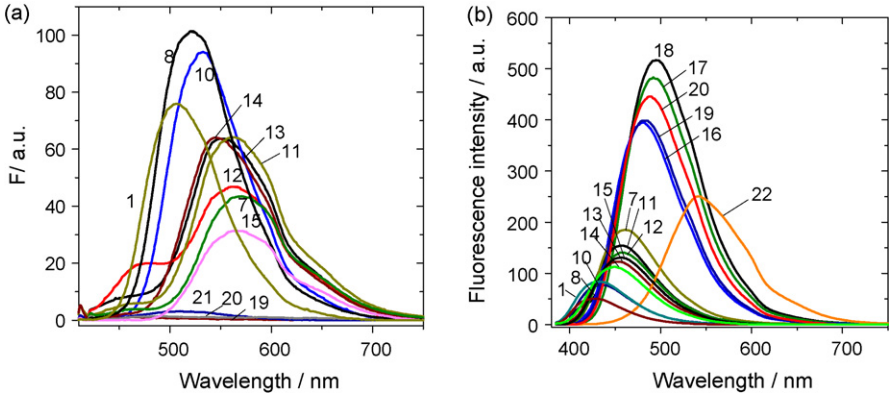

Fig. 2. Selected emission spectra of **4** (a) ($c = 2.11 \times 10^{-5}$ M) and **5** (b) ($c = 2.71 \times 10^{-5}$ M) in several solvents. In order to demonstrate relative fluorescence intensity, the spectra were not normalized. The solvent numbers refer to the solvents in Tables 2 and 3.

Table 1
Photophysical properties of **4** in different solvents[a]

No.	Solvents	λ_{abs} (max/nm)	λ_{em} (max/nm)	$\Delta\nu$ (cm^{-1})	ε ($M^{-1}\,cm^{-1}$)	Φ_f	τ (ns)[b]	k_f ($10^7\,s^{-1}$)	k_{nr} ($10^7\,s^{-1}$)
1	*n*-hexane	393	506	5682	4450	0.080	3.48	2.30	26.4
2	PhMe	401	536	6281	3860	0.113	3.78	2.99	23.5
3	CCl_4	400	443	2427	4148	0.057	2.29	2.49	41.2
4	Benzene	402	537	6254	3960	0.119	4.23	2.81	20.8
5	Dioxane	399	535	6371	4480	0.111	4.22	2.63	21.1
6	NEt_3	398	522	5969	4000	0.103	3.56	2.89	25.2
7	$CHCl_3$	405	571	7178	4770	0.065	3.53	1.84	26.5
8	Et_2O	395	521	6123	4280	0.099	4.03	2.46	22.4
9	EtOAC	395	536	6660	5320	0.085	4.19	2.03	21.8
10	THF	397	532	6392	4990	0.097	4.55	2.13	19.8
11	DCM	404	563	6990	4790	0.078	4.75	1.64	19.4
12	DMSO	406	563	6869	4170	0.060	3.58	1.68	26.3
13	DMF	403	551	6665	4610	0.087	4.82	1.80	18.9
14	Acetone	399	544	6680	4490	0.075	–[c]	–[c]	–[c]
15	MeCN	398	568	7520	4480	0.062	1.85	3.35	50.7
19	EtOH	406	–[d]		4470				
20	MeOH	407	–[d]		4620				
21	H_2O	412	–[d]		3540				

[a] Absorption wavelength (wavelength of first absorption maximum), λ_{abs}; emission wavelength (at the maximum intensity), λ_{em}; Stokes' shifts, $\Delta\nu$; extinction coefficient, ε; fluorescence quantum yields, Φ_f; fluorescence lifetimes, τ; rate constants for radiative fluorescence decay, k_f; rate constants for non-radiative decay, k_{nr}; toluene, PhMe; carbon tetrachloride, CCl_4; 1,4-dioxane, dioxane; triethylamine, NEt_3; chloroform, $CHCl_3$; diethyl ether, Et_2O; ethyl acetate, EtOAc; tetrahydrofuran, THF; dichloromethane, DCM; dimethyl sulfoxide, DMSO; dimethylformamide, DMF; acetonitrile, MeCN. The excitation wavelength for the fluorescence spectra equals to the maximum UV–vis absorption wavelength.

[b] The typical standard error for the lifetime is ±0.01 ns (determined with the fluorescence lifetime spectrometer).

[c] Lifetime was not determined due to the strong absorption of acetone at 300 nm, the wavelength of the excitation light.

[d] No emission in protic solvents.

Table 2
Photophysical properties of compound **5** in different solvents[a]

No.	Solvents	λ_{abs} (max/nm)	λ_{em} (max/nm)	$\Delta\nu$ (cm^{-1})	ε ($M^{-1}\,cm^{-1}$)	Φ_f	τ (ns)[b]	k_f ($10^7\,s^{-1}$)	k_{nr} ($10^7\,s^{-1}$)
1	*n*-Hexane	365	428	4033	16000	0.048	0.64	7.50	149
2	PhMe	374	443	4165	15940	0.086	0.98	8.78	93.3
3	CCl_4	371	443	4381	17560	0.051	0.78	6.54	122
4	Benzene	372	444	4359	21810	0.067	1.16	5.78	80.4
5	Dioxane	373	445	4338	14150	0.103	1.06	9.72	84.6
6	NEt_3	363	433	4454	17690	0.035	0.53	6.60	182
7	$CHCl_3$	376	461	4904	20170	0.171	2.21	7.74	37.5
8	Et_2O	364	437	4589	17920	0.075	0.83	9.04	111
9	EtOAc	366	444	4800	17570	0.097	0.94	10.3	96.1
10	THF	368	441	4498	16090	0.108	1.13	9.56	78.9
11	DCM	373	456	4880	19480	0.132	1.59	8.30	54.6
12	DMSO	374	460	4999	17460	0.146	1.74	8.39	49.1
13	DMF	371	452	4830	15850	0.132	1.69	7.81	51.4
14	Acetone	369	450	4878	19160	0.104	–[c]	–[c]	–[c]
15	MeCN	369	456	5170	18360	0.133	1.96	6.79	44.2
16	Butanol	378	482	5708	18530	0.429	6.64	6.46	8.60
17	Pr-diol	380	492	5991	15500	0.534	9.44	5.66	4.94
18	Et-diol	380	495	6114	15760	0.529	8.95	5.91	5.26
19	EtOH	377	486	5949	14820	0.491	6.33	7.76	8.04
20	MeOH	376	490	6188	15030	0.517	7.38	7.01	6.54
21	H_2O	385	506	6211	13730	0.554	12.1	4.58	3.69
22	HOAc	383	544	7727	15440	0.351	13.4	2.62	4.84

[a] 1-Butanol, butanol; 1,3-propanediol, pr-diol; ethylene glycol, Et-diol; ethanol, EtOH; methanol, MeOH; acetic acid, HOAc.

[b] The typical standard error for the lifetime is 0.01 ns (determined with the fluorescence lifetime spectrometer). For the aprotic solvents, average fluorescence lifetimes were used.

[c] Lifetime was not determined due to the strong absorption of acetone at 300 nm, the wavelength of the excitation light.

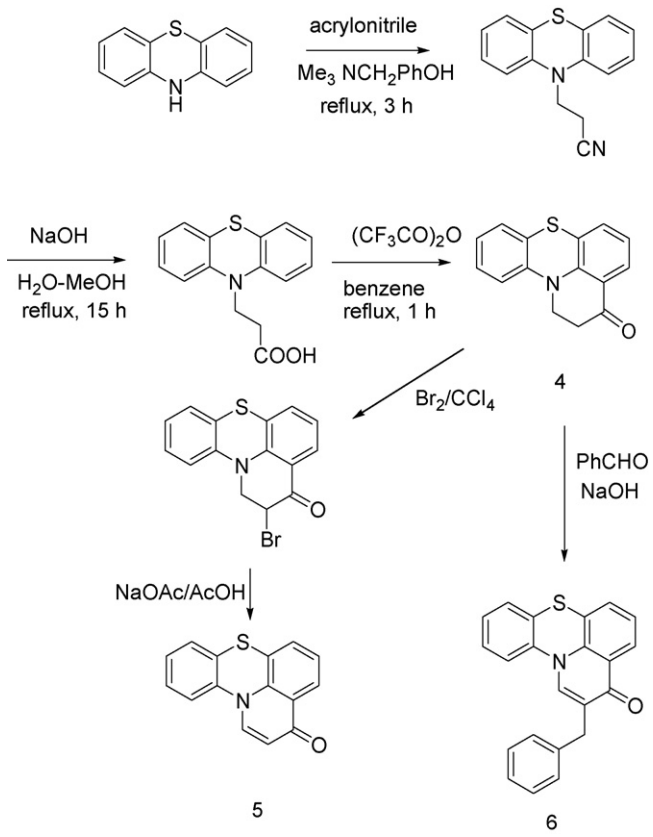

Scheme 2. Synthesis of compounds **4**–**6**.

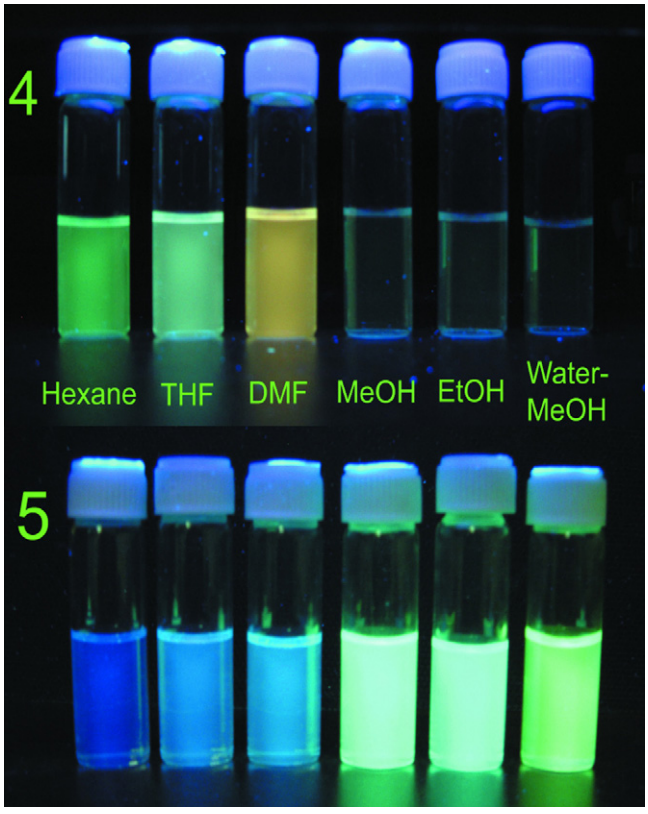

Fig. 3. Visual effect of the polarity sensitivity of the fluorescence of compounds **4** and **5** in solvents of hexane, THF, DMF, MeOH, EtOH, H_2O–MeOH (1:1, v/v). Top row: **4** (2.11×10^{-5} M); bottom row: **5** (2.57×10^{-5} M). Excited with laboratory UV lamp (365 nm).

fluorescence of **4** is quenched in protic solvents, conversely fluorescence of **5** is greatly intensified. **6** shows similar profile to **5** (see supplementary data). The color changes of emission are also discernable. As **4**–**6** are sensitive to the protic solvents and sharp emission changes were observed, therefore, these compounds can be used as polarity probes, such as chemosensor for alcohols or water [3,11].

With fluorescence quantum yields and fluorescence lifetimes, the radiative decay rate constant (k_f) and non-radiative decay rate constant (k_{nr}) of the emission state can be estimated (Eqs. (2a) and (2b)) (with the approximation that only one emission species or one dominant species were observed in neat solvents) [4,34].

$$k_{nr} = \frac{1 - \phi_f}{\tau} \tag{2a}$$

$$k_f = \frac{\phi_f}{\tau} \tag{2b}$$

It was found that increasing the polarity of the solvents leads to the decrease of k_f values of **4** (Table 1). For **5**, however, with increasing the solvent polarity, especially a transition from aprotic solvents to protic solvents, the k_f values almost remain constant, whereas k_{nr} values decrease sharply (Table 2). For example, k_{nr} values decrease from $1.49 \times 10^9\ s^{-1}$ in hexane to $6.54 \times 10^7\ s^{-1}$ in MeOH, but k_f values remain constant, $7.50 \times 10^7\ s^{-1}$ in hexane and $7.01 \times 10^7\ s^{-1}$ in MeOH. This result can be used to partially explain the solvent-dependent emission of the dyes.

The solvent effect on the fluorescence was due to the polarity and especially the hydrogen bond donating ability of the solvents. Considering the structure characters of **4** and **5**, it is proposed that in aprotic solvents, the most probable transition for the compounds is $n \rightarrow \pi^*$ transition, thus the quantum yield is low. For **4**, the hydrogen bonding, especially at the emission state, increase the chance of the non-radiative introversion from the S1 to S0 state, thus the fluorescence was completely quenched in neat protic solvents, such as in MeOH or H_2O [3]. In this case the k_f values decreased. For **5**, however, increasing the solvent polarity, especially the hydrogen bonding donating power of the solvents, leading to the stabilization of the n-orbital of the oxygen in the carbonyl group, will switch the most probable transition from $n \rightarrow \pi^*$ to the $\pi \rightarrow \pi^*$ transition [5].

Radiative emission from $n \rightarrow \pi^*$ states is known to be less efficient than that from $\pi \rightarrow \pi^*$ states [5]. Thus, fluorescence enhancement was observed for **5** in high polar especially protic solvents. For **4** and **5**, a intersystem crossing mechanism for the emission state may be also responsible for the decreased fluorescence intensity, given the excited states with n–π* character are energetically close to the lowest singlet excited sate with π–π* character. However, no n–π* absorption was observed in the UV–vis spectra even at high concentration.

It was found that k_{nr} values of **4** is almost independent of the solvents polarity (Fig. 4. There is correlation between the emission maxima of the dye and the polarity of the solvents).

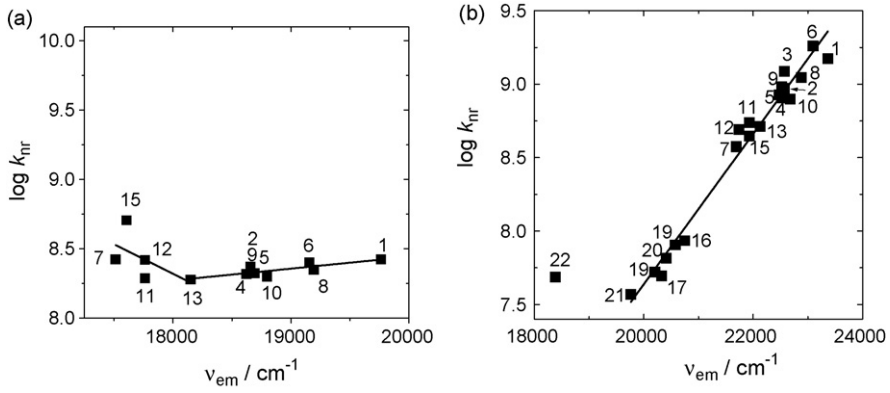

Fig. 4. Plot of log (k_{nr} (s^{-1}) vs. ν_{em} (in cm^{-1}) for **4** (a) and **5** (b). The solid lines represent the linear fitting (for **5**, $r^2 = 0.9760$). Same magnitude of the range of vertical axis were set to clearly compare the correlation between log k_{nr} and ν_{em} of **4** and **5**. Solvent acetic acid, number 22 was not considered for regression of **5**. For the solvent numbers refer to Tables 1 and 2.

Table 3
Selected photophysical properties of **6** in several solvents

Solvents	λ_{abs} max (nm)	λ_{em} max (nm)	ε (M^{-1} cm^{-1})	Φ_f	τ[a] (ns)
Et_2O	374	442	6300	0.114	1.86
THF	378	453	8520	0.126	1.54
DCM	380	461	8660	0.184	2.11
MeCN	377	460	6170	0.208	1.95
1-Butanol	383	485	8490	0.539	5.51
EtOH	381	486	5860	0.781	6.32
MeOH	384	491	6800	0.739	7.24
H_2O	395	492	7770	0.235	1.07

[a] The typical standard error for the lifetime is ±0.01 ns (determined with the fluorescence lifetime spectrometer).

However, a transition is observed at $\Delta f = 0.2$ (Δf is the solvent polarity scale of orientation polarizability, refer to Sections 2.1 and 3.3), this may be due to the charge transfer character of **4** in solvents with higher polarity [34]. For **5**, however, increasing the polarity of solvents leads to decrease of k_{nr} values (Fig. 4). The strong linear correlation between log k_{nr} values and emission maxima (ν_{em}) of **5** is most possibly due to the suppression of the non-radiative decay (such as internal conversion) by the interaction with the protic solvents [30]. This is consistent with the assumption of switching from $n \rightarrow \pi^*$ transition to $\pi \rightarrow \pi^*$ transition with increasing of the solvent polarity, especially switching from aprotic solvents to the protic solvents. However, more investigation is needed to elucidate the different photophysical properties of compound **4** or **5**. It is interesting that **4** and **5** gives emissions at about 500 nm, considering their relatively limited π-electron delocalization system [30,35]. As the emission of the compounds are strongly solvent dependent, therefore, the solvatochromism of these compounds are studied in more detail.

3.3. Lippert–Mataga correlation of the Stokes' shifts

Solvent effects on the photophysical properties of dyes are due to their interaction with the microenvironment (such as the solvation cage) in solution, via the dipole–dipole interaction, hydrogen bond, charge transfer, the re-orientation of the dipole moments of the solvents upon excitation of the fluorophores, etc. [4,5]. General solvent effect and specific solvent effect are used to describe the solvatochromic properties. It should be noted that besides the solvents effect, the intrinsic origin for the Stokes' shift is the structural relaxation of the molecular skeleton at the excited-state (such as the non-radiative decay from the vibrationally excited-state to the vibrational ground-state, both are the electronically excited-state, such as S1).

The simplest consideration for general solvent effect is the Lippert–Mataga equation (Eqs. (3a) and (3b)), by assuming that same excited-state is involved in absorption and emission, and energy difference between the ground- and excited-state is only proportional to solvent orientation polarizability (Δf) [4,5].

$$\Delta\nu = \frac{2\Delta f}{4\pi\varepsilon_0 hca^3}(\mu_e - \mu_g)^2 + \text{constant} \tag{3a}$$

$$\Delta f = \frac{\varepsilon - 1}{2\varepsilon + 1} - \frac{n^2 - 1}{2n^2 + 1} \tag{3b}$$

where $\Delta\nu = \nu_{abs} - \nu_{em}$ stands for Stokes' shift, ν_{abs} and ν_{em} are absorption and emission (cm^{-1}), h is the Planck's constant, c is the velocity of light in vacuum, a is the radius of the solvent cavity in which the fluorophore resides (Onsager cavity radius) [4,5,21,36]. Δf is the orientation polarizability, μ_e and μ_g is the ground-state dipole in the ground-state geometry and the excited dipole in the excited-state geometry and ε_0 is the permittivity of the vacuum [4,5].

The Lippert–Mataga correlations of the Stokes' shifts of compounds **4** and **5** are depicted in Fig. 5. Poor linearity was found for the overall regression for both **4** and **5**. For **5**, clearly the aprotic and protic solvents divided into two isolated domains in the plot. Similar result as also observed for **6** (see supplementary data). Such an isolation of the protic and aprotic solvents in the Lippert–Mataga plots are typical for polarity probes, such as PRODAN and its analogue reported recently [1,5,37]. Exclusive regressions of the two isolated domains of the aprotic and protic solvents gives good linearity (see supplementary data).

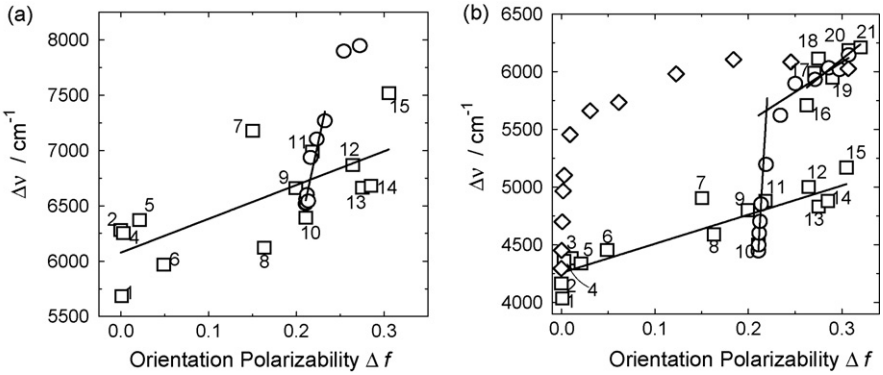

Fig. 5. Lippert–Mataga regressions of compounds **4** (a) and **5** (b): Stokes' shifts (cm^{-1}) of compounds vs. the Lippert solvent parameters of orientation polarizability (Δf). Binary solvents are included: THF–MeOH, open circles; PhMe–MeOH, open diamonds. The solid lines represent the linear regressions. The numbers refer to the solvents in Tables 1 and 2.

The Δf values of MeCN, DMF and acetone are similar to the protic solvents, such as MeOH, EtOH and water, but the Stokes' shifts of **5** in MeCN are much smaller than that in MeOH, indicates a specific solvent effect with protic solvents [4,37]. Because Lippert–Mataga consideration is devoid of chemical interactions, so this model cannot be used to explain a specific solvent–fluorophore interaction [4]. Thus, the non-linearity of the Lippert–Mataga correlation indicates a specific solvent effect, most probably intermolecular hydrogen bonding between the solutes and the solvents molecules [4,5,37]. This assumption is supported by the calculated molecular orbitals of **4** (see supplementary data).

In order to prove this specific solvent effect of hydrogen bonding, binary solvents (THF–MeOH and PhMe–MeOH) were also used in the Lippert–Mataga plotting (Fig. 5). With introduction of small amount of MeOH to the THF solution of the compounds, the Stokes' shifts of **4** or **5** changes drastically. This sharp increase (bursting character) is not likely due to the polarity change of the bulky solvents because the amount of MeOH added is very small at this stage [4,21]. Therefore, a specific rather than general solvent effect exists in the presence of MeOH. However, the difference between the Δf values of THF and MeOH is small, thus, in order to eliminate the possible artificial bursting character of this binary system, another binary solvent of toluene–MeOH was used, for which the difference of the Δf values of the two neat solvents is big enough to observe the intrinsic bursting character of the variation of Stokes' shifts. With increasing the MeOH content in the mixed solvents, the Stokes' shifts can either increase linearly with the same slope to that of the neat aprotic solvents, which indicates a general solvent effect, or firstly give a sharp increase of the Stokes' shift, then to join the protic solvent domain through a plateau, which will be a strong evidence of specific solvent effect of hydrogen bonding.

The results show that introduce of small amount of MeOH to toluene solution of **5** leads to a dramatic increase of the Stokes' shift of **5** (Fig. 5b), which clearly indicated the specific solvent effect, most probably the hydrogen bonding between the solute and the solvent molecules. A further negative control to prove this specific solvent effect was carried out by using toluene–DMF binary solvents (see supplementary data). Despite of the strong hydrogen bond accepting ability, DMF is not a hydrogen bond donor thus it cannot form hydrogen bond with the molecules of compound **5**, therefore, no bursting phase should be observed with increasing the DMF ratio in its binary mixture with toluene, which was proved with experiment results (see supplementary data).

Besides emission spectra, UV–vis absorption spectra of the compounds also show minor solvent dependence (see supplementary data), thus, it is proposed that the hydrogen bonding does occur at the ground-state, but it is more significant at the emission state.

3.4. Estimated dipole moment changes of *4* and *5* with excitation

From the slops of Lippert–Mataga plots (Fig. 5), dipole moment changes of **4** and **5** with excitation were estimated with Eq. (3a) (see supplementary data). The Onsager radius (a) is estimated with the single crystal structure by assuming that charge transfer occurred mainly in the direction from sulfur atoms (donor) to oxygen of the carbonyl group (acceptor) (see supplementary data).

The dipole moment changes ($\Delta\mu_{ge}$) of **4** and **5** are similar to the reported polarity probes [5,34]. The $\Delta\mu_{ge}$ values in the protic solvents are found to be higher than that in aprotic solvents. For example, the $\Delta\mu_{ge}$ of **5** is 7.9 ± 3.2 D in protic solvents, whereas the value is only 4.9 ± 0.7 D in aprotic solvents. **4** gives a slightly higher dipole moment change than **5** (see supplementary data).

These dipole moment changes are comparable to that of the well-known polarity probe such as PRODAN, which gives a value of about 7–8 D [5]. We demonstrated that the specific solvent effect of hydrogen bonding is responsible for the solvent sensitivity of the polarity probes, despite of the modest dipole moment change with excitation. This is also true for PRODAN [5]. The initially reported very high dipole moment change of 20 D for PRODAN was suggested to be overestimated [1,5].

3.5. Correlation of the Stokes' shifts with $E_T^N(30)$ values

As Lippert–Mataga regression assumes that Stokes' shift is only dependent on orientation polarizability of the solvents, which is clearly not applicable for **4** and **5**, thus its failure to give linear regression on the photophysical data of **4** and **5** indicates a specific solvent effect [4,5]. In this case, a better description of the solvatochromism can be established by using the solvent scales for which the contributions of specific solvent effects, such as hydrogen bonding, are considered. Thus, the Stokes' shifts were correlated with the normalized molar electronic transition energies, the $E_T^N(30)$ values [15].

The correlations between Stokes' shift of **4** and **5** and $E_T^N(30)$ values of the solvents are depicted in Fig. 6. A much better linearity than that of the Lippert–Mataga plots was observed. For **5**, the linear plot comprises all the solvents, even the protic solvents such as MeOH that show sever deviation in the Lippert–Mataga correlation. This result is different from a polarity sensitive borondipyrromethene dye, for which the linear plot of Stokes' shifts vs. $E_T^N(30)$ values failed to comprise the protic solvents [34].

The satisfying regression of the solvent dependence of the Stokes' shift by $E_T^N(30)$ scales, and the failure of the Lippert–Mataga correlation to do so, together with the profiles of the Lippert–Mataga plots for binary solvents (Fig. 5), gives strong evidence that the hydrogen bonding is essential for the solvent dependency of the emissions of **4** and **5**.

3.6. Multilinear regression of the photophysical properties with Catalán and Kamlet–Taft scales

The solvent dependency of the photophysical properties of a dye, such as ν_{abs}, ν_{em} and Stokes' shifts ($\Delta\nu$, in cm^{-1}) can also be described with multilinear regression by the following equation:

$$y = y_0 + aA + bB + cC \quad (4)$$

where y is the photophysical property (such as absorption, emission maxima or Stokes' shifts, in cm^{-1}), y_0 stands for the intrinsic photophysical property of the dye in the absence of solvents (i.e. in vacuum) and A, B and C stands for the characteristic parameters of the solvents. a, b and c are the adjustable coefficients that determine the contribution of the respective parameters of the solvents (A, B or C) to the photophysical property of the dye (y).

The popular solvents scales for multilinear correlation are the Catalán [16–19], and Kamlet–Taft scales [20]. For both of these scales, the acidity, basicity and the polarity/polarizability of the solvents are considered. For the Catalán scales, the parameters are termed as SA, SB and SPP, respectively. Whereas for the Kamlet–Taft scales, the parameters are termed as α, β, and π^*. Thus the multilinear regression can be described as

$$y = y_0 + a_{SA} \times SA + b_{SB} \times SB + c_{SPP} \times SPP \quad (Catalán)(4a)$$

$$y = y_0 + a_\alpha \alpha + b_\beta \beta + c_{\pi*} \pi^* \quad (Kamlet–Taft) \quad (4b)$$

Through the multilinear regression of the photophysical data, the coefficients y_0, a_{SA}, b_{SB} and c_{SPP}, or a_α, b_β, and $c_{\pi*}$ can be obtained simultaneously, so that the contribution of the respective property of the solvents, i.e. the acidity (SA or α), basicity (SB or β) or the polarity/polarizability (SPP or π*), to the photophysical property of the dye can be evaluated. Thus the multilinear regression is helpful to reveal the origin of the solvent sensitivity of the solvatochromic/solvatofluorochromic dyes.

The multilinear regression of the photophysical data of **4** and **5** were conducted and the result of **5** was compiled in Table 4 (data of **4** is available, see supplementary data). It was found that the absorption, emission maxima and Stokes' shifts are solvent-dependent. The absorption show only modest correlation to the solvents parameters, but the emission and Stokes' shifts show much stronger correlation, evaluated by the absolute values of the coefficients [34]. This is also proved by the UV–vis absorption spectra and the fluorescence spectra (Figs. 1 and 2).

It was found for compound **4** or **5**, the regression with either the Catalán or the Kamlet–Taft solvent scales gives similar y_0 values. This means the predicted intrinsic photophysical properties of the dye **4** or **5** by the two model is similar. However, different coefficients for solvent acidity, basicity and polarity/polarizability are obtained with the two models. The Kamlet–Taft scales give better regression than the Catalán scales (r^2 and the standard errors of the parameters as the evaluation criteria), this is different from the result of a solvatofluorochromic borondipyrromethene dye [34]. For the regression of the emission, with the Kamlet–Taft scales, most r^2 values are higher than 0.95. Conversely, the r^2 values for the Catalán regression are usually smaller than 0.90. Furthermore, the standard errors for the parameters obtained with the Kamlet–Taft regression are also smaller. However, a conclusion cannot be drawn from these results that the Kamlet–Taft scales are universally *better* or more *reliable* than the Catalán scales.

In order to investigate the respective effect of the acidity, basicity and polarity/polarizability on the photophysical properties exclusively, regressions with less parameters were carried out. The β-independent regression gave similar y_0, a_α and $c_{\pi*}$ values to the regressions with full parameters, hydrogen bond donating capability of the solvents, instead of the hydrogen bond accepting capability (i.e. the basicity), is more definitive for the emission of **4** and **5**. From Table 4, it can be found that for the emission and the Stokes' shifts, the contribution from the acidity, basicity of the solvents are unequally weighted, demonstrated by the acidity- or basicity-independent regressions of the photophysical data as well as the absolute values of the respective coefficients. For example, the coefficients of the emission and the Stokes' shifts show that the absolute a_α values (or a_{SA}) are nearly 10 times higher than the b_β (or b_{SB}) values. For the absorption of the compounds, however, the coefficients for the acidity of the solvents (a_α or a_{SA}) is only two-fold of the coefficients of the basicity of the solvents (b_β or b_{SB}). Moreover, the magnitude of the coefficients for the acidity and the polarity–polarizability for absorption is only 10–50% of the corresponding coefficients for emission. These results indicated that the hydrogen bond donating capability of the solvents is more definitive than the basicity of the solvents on the emission of the compounds, and

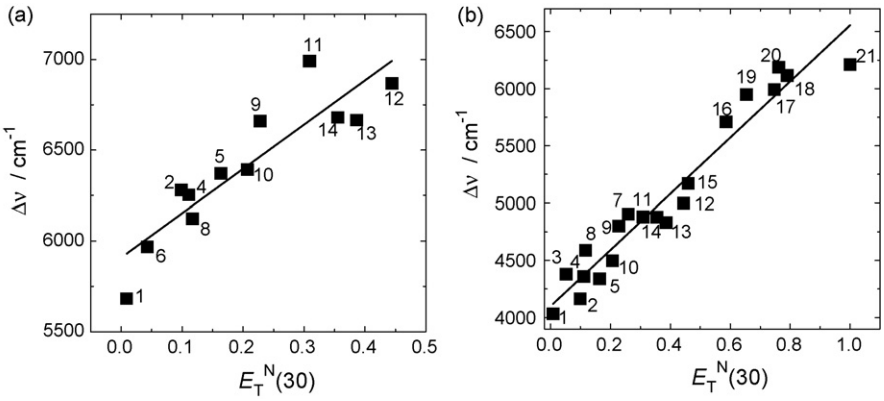

Fig. 6. Stokes' shifts ($\Delta\nu$) of compounds **4** (a) and **5** (b) vs. $E_T^N(30)$ values of the solvents. The solid lines represents the linear regressions of the experimental data (**4**, $r^2 = 0.8124$; **5**, $r^2 = 0.9443$). The solvent numbers refer to the solvents in Tables 1 and 2.

the hydrogen bond interaction is stronger at the emission state. Further evidence comes from the perfect linear correlation of the photophysical properties with $E_T^N(30)$ scales, a solvent scale that hydrogen-bonding effect is considered. Moreover, although the solvatochromism exists at the ground-state (from UV–vis spectra), yet the solvent-dependency is more significant for the emission state. This observation is supportive for the strong hydrogen bonding at the excited-state.

In order to clearly demonstrate the quality of the multilinear regressions, the correlation between the predicted fluorescence emission maxima (cm^{-1}) by the multilinear regression (using the estimated *a*, *b* and *c* parameters) vs. the experimental values was depicted in Fig. 7. The linearity of the curves is directly correlated to the multilinear regression quality. For compound **4** (Fig. 7a and b), a strong linear correlation between the predicted and experimental results was observed. For **5**, the protic and the aprotic solvents separated into two isolated domains, each with good linearity but different slopes (Fig. 7c and d).

Separate regression of the two isolated domains of solvents (shown in Fig. 7c and d) were conducted with Catalán and Kamlet–Taft scales and better regression was resulted (see supplementary data). It also reveals that the y_0 value is similar in aprotic and protic solvents, but the estimated coefficients (acidity or basicity) for the aprotic and protic solvents are different (see supplementary data).

The multilinear regression were also conducted for the absorption of **4** and **5**, a strong correlation was found (Table 4 and Fig. 8) (see supplementary data). It is proposed that inter-

Table 4
Estimated Coefficients (y_0, *a*, *b*, *c*; see Eq. (4)), standard errors and correlation coefficients (r^2) for the multilinear regression analysis of the absorption (ν_{abs}), fluorescence emission maxima (ν_{em}) and the Stokes' shift ($\Delta\nu = \nu_{abs} - \nu_{em}$) of compound **5** in solvents as a function of the Catalán (Eq. (4a); acidity SA, basicity SB, and polarity/polarizability SPP) and Kamlet–Taft (Eq. (4b); acidity α, basicity β and polarity/polarizability π*) solvent scales

Catalán	y_0 (cm^{-1})	a_{SA}	b_{SB}	c_{SPP}	r^2
ν_{abs}	$(2.77 \pm 0.03) \times 10^4$	$(-8.50 \pm 2.01) \times 10^2$	$(4.05 \pm 2.05) \times 10^2$	$(-1.04 \pm 0.48) \times 10^3$	0.7345
ν_{abs}	$(2.76 \pm 0.04) \times 10^4$	$(-9.16 \pm 2.13) \times 10^2$	–[a]	$(-7.38 \pm 4.85) \times 10^2$	0.6734
ν_{abs}	$(2.83 \pm 0.04) \times 10^4$	–[a]	$(5.49 \pm 2.81) \times 10^2$	$(-2.11 \pm 0.56) \times 10^3$	0.4545
ν_{em}	$(2.46 \pm 0.05) \times 10^4$	$(-2.54 \pm 0.03) \times 10^3$	$(-0.25 \pm 3.10) \times 10^2$	$(-2.82 \pm 0.71) \times 10^3$	0.9046
ν_{em}	$(2.46 \pm 0.05) \times 10^4$	$(-2.53 \pm 0.29) \times 10^3$	–[a]	$(-2.84 \pm 0.66) \times 10^3$	0.9046
ν_{em}	$(2.65 \pm 0.01) \times 10^4$	–[a]	$(4.05 \pm 6.56) \times 10^2$	$(-6.01 \pm 1.29) \times 10^3$	0.5372
$\Delta\nu$	$(3.23 \pm 0.38) \times 10^3$	$(1.71 \pm 0.24) \times 10^3$	$(4.38 \pm 2.24) \times 10^2$	$(1.61 \pm 0.52) \times 10^3$	0.8800
$\Delta\nu$	$(3.17 \pm 0.42) \times 10^3$	$(1.62 \pm 0.25) \times 10^3$	–[a]	$(1.93 \pm 0.54) \times 10^3$	0.8494
$\Delta\nu$	$(2.23 \pm 0.73) \times 10^3$	–[a]	$(1.17 \pm 4.48) \times 10^2$	$(3.34 \pm 0.94) \times 10^3$	0.4668
Kamlet–Taft	y_0 (cm^{-1})	a_α	b_β	c_{π^*}	r^2
ν_{abs}	$(2.73 \pm 0.01) \times 10^4$	$(-7.10 \pm 1.13) \times 10^2$	$(3.63 \pm 1.80) \times 10^2$	$(-6.43 \pm 1.73) \times 10^2$	0.7928
ν_{abs}	$(2.74 \pm 0.01) \times 10^3$	$(-6.19 \pm 1.34) \times 10^2$	–[a]	$(-6.10 \pm 1.88) \times 10^2$	0.7362
ν_{abs}	$(2.74 \pm 0.02) \times 10^3$	–[a]	34.7 ± 281	$(-8.78 \pm 2.78) \times 10^2$	0.3894
ν_{em}	$(2.32 \pm 0.01) \times 10^4$	$(-2.03 \pm 0.12) \times 10^3$	$(-1.59 \pm 1.77) \times 10^2$	$(-1.14 \pm 0.17) \times 10^3$	0.9702
ν_{em}	$(2.31 \pm 0.01) \times 10^4$	$(-2.06 \pm 0.12) \times 10^3$	–[a]	$(-1.15 \pm 0.17) \times 10^3$	0.9687
ν_{em}	$(2.36 \pm 0.05) \times 10^4$	–[a]	$(-1.11 \pm 0.68) \times 10^3$	$(-2.04 \pm 0.65) \times 10^3$	0.4708
$\Delta\nu$	$(4.12 \pm 0.10) \times 10^3$	$(1.32 \pm 0.11) \times 10^3$	$(5.11 \pm 1.56) \times 10^2$	$(4.73 \pm 1.50) \times 10^2$	0.9446
$\Delta\nu$	$(4.29 \pm 0.11) \times 10^3$	$(1.45 \pm 0.14) \times 10^3$	–[a]	$(5.18 \pm 1.90) \times 10^2$	0.9050
$\Delta\nu$	$(3.91 \pm 0.31) \times 10^3$	–[a]	$(1.12 \pm 0.45) \times 10^3$	$(9.12 \pm 4.45) \times 10^2$	0.4475

[a] The corresponding solvent parameters are not considered for the regression so that the dependency of the emission of compound **5** on the respective parameters of the solvents can be evaluated exclusively.

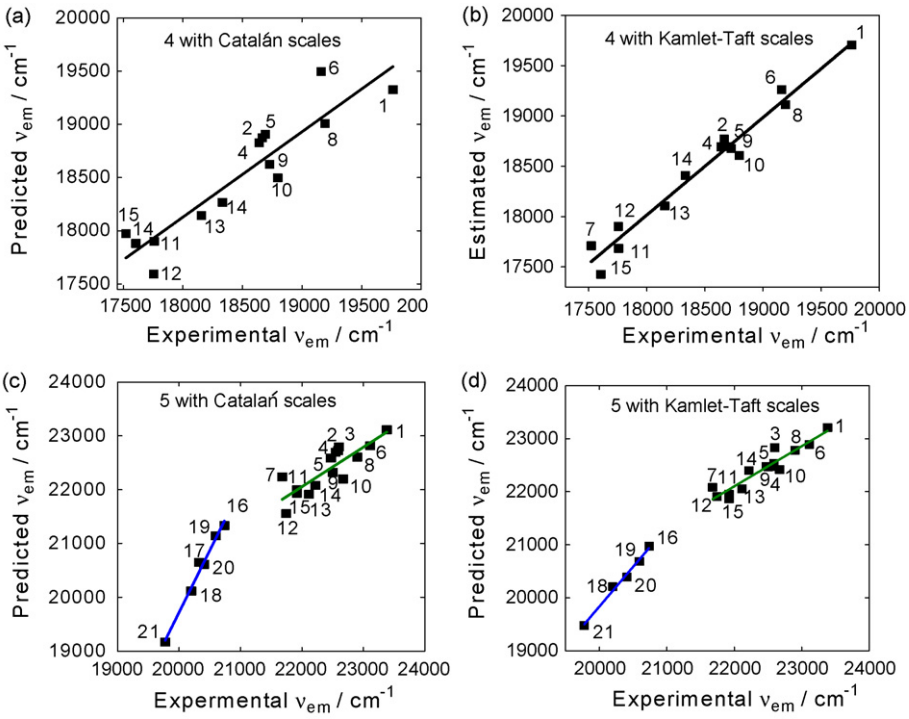

Fig. 7. Linear relationship between the experimental and predicted fluorescence emission maxima ν_{em} (in cm^{-1}) of **4** and **5** obtained by multilinear regression according to Eqs. (4a) and (4b), in which the parameters a, b and c are estimated simultaneously. The regression of **4** with (a) Catalán scales (fitting goodness $r^2 = 0.8829$) and (b) Kamlet–Taft scales ($r^2 = 0.9695$); (c) the regression of **5** with Catalán scales (for the fitting of protic and aprotic solvents, $r^2 = 0.9989$ and 0.8641, respectively); (d) the regression of **5** with Kamlet–Taft scales (for the fitting of protic and aprotic solvents, $r^2 = 0.9983$ and 0.9041, respectively). Regression for different solvents: protic solvents, blue lines; aprotic solvents, dark green lines. The solid lines represent the linear fitting. The numbers refer to the solvents in Tables 1 and 2.

action between the compound and the solvent molecules exists at ground-state.

The multilinear regressions of the Stokes' shifts of **5** show that there is no isolated solvent domains in the plots (see supplementary data). It is proposed that the solvents isolation in Fig. 7c and d are due to the lacking of the absorption factors in the emission regression. As the absorption of **4** and **5** are also solvent-dependent (Table 4 and Fig. 8), only to less extent compared to the emission, thus it should be considered in the regression. As a proof of this assumption, linear correlation of the Stokes shifts of **5** was carried out and no drastic solvent isolations are found in the plots because the Stokes' shifts contains both the absorption and the emission information.

The exact reason for the better regression result with Kamlet–Taft scales than the Catalán scales in the present case of compounds **4** and **5** is still unclear. However, it should be kept in mind that the solvent effects observed for a given probe, for instance the solvent parameters, should not be readily transferable to any other solute, particularly the probes contain different functional groups [16]. From Table 4 (compound **5**), it was found that both Kamlet–Taft and Catalán scales give similar y_0 value, but two scales give different results for the effect

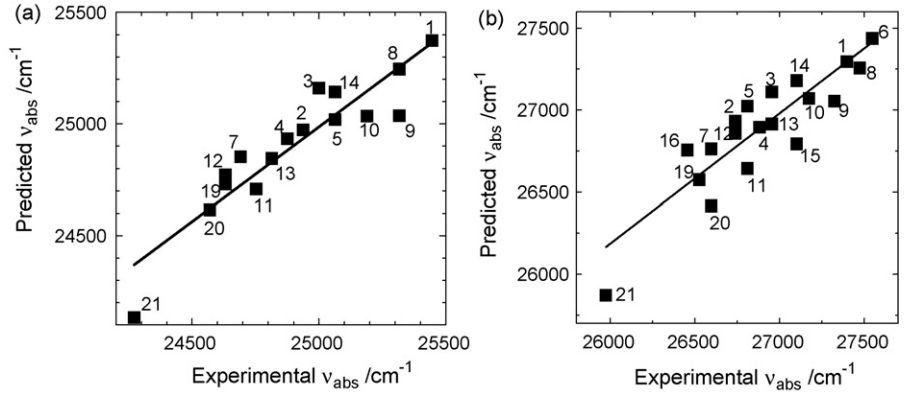

Fig. 8. Linear relationship between the experimental and the predicted absorption ν_{abs} (in cm^{-1}) of **4** (a) and **5** (b) obtained by multilinear regression with Kamlet–Taft scales, according to Eq. (4b), in which the parameters a_α, b_β and c_{π^*} are estimated simultaneously. The solid lines represent the linear fitting. The numbers refer to the solvents in Tables 1 and 2.

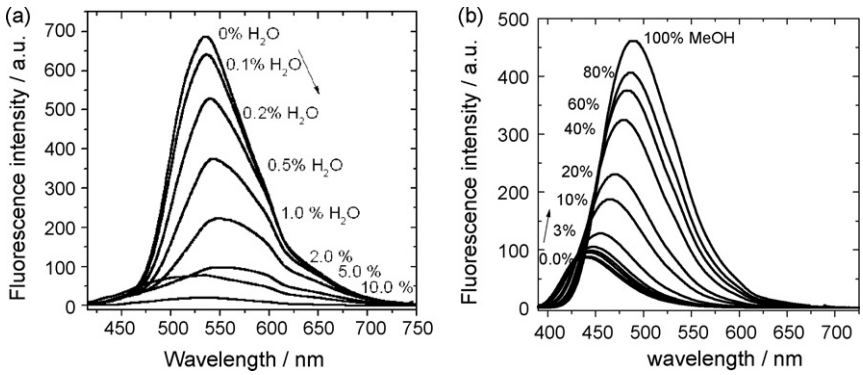

Fig. 9. Variation of the fluorescence spectra of the compounds **4** and **5** in aprotic solvents titrated with protic solvents. (a) Spectra of compound **4**, with addition of H_2O to THF solution, $\lambda_{ex} = 397$ nm; (b) fluorescence spectra of **5**, with addition of MeOH to THF solution, $\lambda_{ex} = 368$ nm.

of solvent acidity and basicity on the photophysical properties. However, it is not safe to draw a conclusion from these results that the Kamlet–Taft scales are *universally* better than the Catalán scales. The regression quality of the two models will vary from compounds to compounds. For example, it is reported that the Catalán scales give better regression than the Kamlet–Taft scales for a borondipyrromethene dye [34].

3.7. Fluorescence intensity in binary solvents

The emission intensity of **4** and **5** are extremely sensitive to the presence of protic solvents, such as MeOH or water (Fig. 9). With 2% water (v/v) was added to the THF solution of **4**, the fluorescence intensity of **4** was quenched by 60%. Similar quenching effect was also observed with addition of MeOH (see supplementary data). Stern–Volmer equation in which both the static and dynamic quenching are considered, is used to describe the quenching effect (Eq. (5)).

$$\frac{F_0}{F} = 1 + (K_D + K_S)[Q] + K_D K_S [Q]^2 \quad (5)$$

where F_0 is the fluorescence intensity of the dye, F is the fluorescence intensity in the presence of quencher, [Q] is the molar concentration of the quencher and K_S, K_D are the quenching constants of static and the dynamic quenching effect, respectively. For **4** and **5**, strong solvent effects of hydrogen bonding exist, therefore the concentration of the interaction species in the solvent cage is different from the macroscopic concentration. Thus, an approximation has to be employed and the following equation was used to quantitatively evaluate the sensitivity of **4** to water [4,5].

$$\frac{F_0}{F} = 1 + K_{app}[Q] \quad (6)$$

For compound **4**, the Stern–Volmer plotting is linear at low-water concentration (see supplementary data). This is reasonable considering that the specific solvent effect of hydrogen bonding is responsible for the burst phase. An apparent quenching constant of $K_{app} = (1.35 \pm 0.04) \times 10^3\ M^{-1}$ ($r^2 = 0.9964$) was determined for water. With MeOH, similar quenching effect was observed $K_{app} = (1.46 \pm 0.03) \times 10^3\ M^{-1}$ ($r^2 = 0.9967$) (see supplementary data).

Compound **5** gives red-shifted emission with more MeOH added, but for the excitation spectra, no significant red-shifts were observed (see supplementary data). Interestingly, addition of water or MeOH to the solution of **5** in aprotic solvents will significantly enhance the fluorescence (Fig. 9b). This photophysical property is different from most of the normal polarity probes which are less fluorescent in more polar solvents [3,4,33,38,39]. Much attention has been paid to this kind of novel fluorophores with reversed polarity sensitivity [11].

As the fluorescence of **4** and **5** are extremely sensitive to protic solvents, such as water and alcohols, thus these compounds can be used as alcohol sensors, or to detect the trace water in organic solvents, such as in acetone, diethyl ether or THF, etc. [3].

3.8. pH dependence of the fluorescence

The nitrogen atom in compound **5** can be protonated or deprotonated by variation of the pH of the solution, thus the pH dependence of **5** was studied (Fig. 10). As the fluorescence of compound **4** is severely quenched in aqueous solution, therefore, no pH-dependency study was carried out for this compound.

The emission of **5** in aqueous MeOH is proved to be pH-independent in the pH range of 4–11 (Fig. 10), whereas the fluorescence intensity was reduced by about 50% with the pH decrease from 4 to 2. This property is different from a borondipyrromethene dye polarity probe [33].

The pH-independency of the emission of **5** in physiological pH range, as well as the intensified, red-shifted emission in protic solvents, are valuable photophysical properties for this compound to be used as polarity probes, such as membrane probes [4].

4. Conclusion

1,10-Fused ring phenothiazine derivatives **5** and **6** were demonstrated to be a new kind of solvent sensitive fluorescent dyes that strongly fluorescence in protic solvents than in aprotic solvents. A subtle variation of the molecular structure causes complete switching effect on the solvents sensitivity, i.e. compound **4** is fluorescent in aprotic solvents but non-fluorescent in protic solvents. The linear correlation of the photophysical data with the solvent properties can be well established

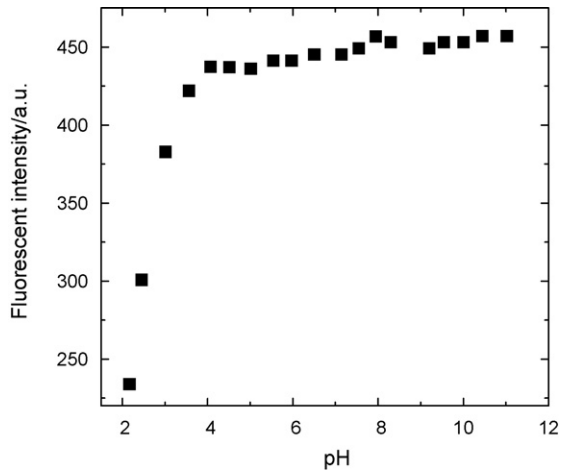

Fig. 10. pH-Dependence of the fluorescence intensity of **5**. $c = 2.58 \times 10^{-5}$ M in 0.05 M NaCl ionic buffer (50% MeOH in H_2O, v/v). $\lambda_{ex} = 395$ nm and $\lambda_{em} = 500$ nm.

with $E_T^N(30)$ scales, whereas the Lippert–Mataga correlation failed to give linear plots, indicating a specific solvent effect. Multilinear regression study of the solvatochromism was also conducted with the Kamlet–Taft and Catalán solvent scales. It was found that the Kamlet–Taft scales give a better regression than the Catalán scales. The results suggested a hydrogen bonding mechanism for the specific solvent effect of the compounds, especially at the emission state. In principle, this kind of polarity fluorophore can be used as sensitive, complementary polarity probes to study the interaction of the solutes with microenvironment, such as to probe the hydrophilicity of the binding pocket of enzyme inhibitor, or the microenvironment in biological membranes. Our future aim is to prepare the derivatives of **5** to gain higher fluorescence quantum yields, longer emission wavelength and especially a more distinct OFF-ON character of the fluorescence with switching from aprotic solvents to protic solvents, and to explore the application of the 1,10-fused ring phenothiazines as molecular probes, such as polarity probes, or as fluorescent dyes for non-covalent detection of proteins and as fluorophores for chemosensors.

Acknowledgements

This work is financially supported by the National Natural Science Foundation of China (NSFC 20634040, 20642003), Scientific Research Foundation for the Returned Overseas Chinese Scholars (Ministry of Education), Science Research Foundation of Dalian University of Technology and French CNRS GDRI 'PHENICS' no. 93. The authors are grateful to Dr. Cheng He for single crystal structure analysis and Dr. Jingxi Pan for his assistance in the fluorescence lifetime measurement.

Appendix A. Supplementary data

Supplementary data associated with this article can be found, in the online version, at: doi:10.1016/j.jphotochem.2007.11.007.

References

[1] G. Weber, F.J. Farris, Biochemistry 18 (1979) 3075–3078.
[2] J.F. Callan, A.P. de Silva, D.C. Magri, Tetrahedron 61 (2005) 8551–8588.
[3] D. Citterio, K. Minamihashi, Y. Kuniyoshi, H. Hisamoto, S. Sasaki, K. Suzuki, Anal. Chem. 73 (2001) 5339–5345.
[4] J.R. Lakowicz, Principles of Fluorescence Spectroscopy, 2nd ed., Kluwer Academic/Plenum Publishers, New York, 1999.
[5] B. Valeur, Molecular Fluorescence: Principles and Applications, Wiley–VCH Verlag GmbH, 2001.
[6] E. Vaganova, S. Yitzchaik, M. Sigalov, J.W. Borst, A. Visser, H. Ovadia, V. Khodorkovsky, New J. Chem. 29 (2005) 1044–1048.
[7] S. Trupp, A. Schweitzer, G.J. Mohr, Org. Biomol. Chem. 4 (2006) 2965–2968.
[8] G. Heinrichs, M. Schellentraeger, S. Kubik, Eur. J. Org. Chem. 18 (2006) 4177–4186.
[9] X. Poteau, A.I. Brown, R.G. Brown, C. Holmes, D. Matthew, Dyes Pigments 47 (2000) 91–105.
[10] M.E. Vazquez, J.B. Blanco, B. Imperiali, J. Am. Chem. Soc. 27 (2005) 1300–1306.
[11] S. Uchiyama, K. Takehira, T. Yoshihara, S. Tobita, T. Ohwada, Org. Lett. 8 (2006) 5869–5872.
[12] A. Kellmann, J. Phys. Chem. 81 (1977) 1195–1198.
[13] K. Kalyanasundaram, J.K. Thomas, J. Phys. Chem. 81 (1977) 2176–2180.
[14] J.S.S. de Melo, R.S. Becker, A.L. Macanita, J. Phys. Chem. 98 (1994) 6054–6058.
[15] C. Reichardt, Chem. Rev. 94 (1994) 2319–2358.
[16] Y. Marcus, Chem. Soc. Rev. (1993) 409–416.
[17] J. Catalán, J. Org. Chem. 62 (1997) 8231–8234.
[18] G. Wypych (Ed.), Handbook of Solvents, ChemTec Publishing, Toronto, Canada, 2001, pp. 583–616.
[19] J. Catalán, J. Palomar, C. Diaz, J.L.G. de Paz, J. Phys. Chem. A 101 (1997) 5183–5189.
[20] M.J. Kamlet, R.W. Taft, J. Am. Chem. Soc. 98 (1976) 377–383.
[21] S.Y. Fung, J. Duhamel, P. Chen, J. Phys. Chem. A 110 (2006) 11446–11454.
[22] M.J. Frisch, G.W. Trucks, H.B. Schlegel, G.E. Scuseria, M.A. Robb, J.R. Cheeseman Jr., J.A. Montgomery, T. Vreven, K.N. Kudin, J.C. Burant, J.M. Millam, S.S. Iyengar, J. Tomasi, V. Barone, B. Mennucci, M. Cossi, G. Scalmani, N. Rega, G.A. Petersson, H. Nakatsuji, M. Hada, M. Ehara, K. Toyota, R. Fukuda, J. Hasegawa, M. Ishida, T. Nakajima, Y. Honda, O. Kitao, H. Nakai, M. Klene, X. Li, J.E. Knox, H.P. Hratchian, J.B. Cross, C. Adamo, J. Jaramillo, R. Gomperts, R.E. Stratmann, O. Yazyev, A.J. Austin, R. Cammi, C. Pomelli, J.W. Ochterski, P.Y. Ayala, K. Morokuma, G.A. Voth, P. Salvador, J.J. Dannenberg, V.G. Zakrzewski, S. Dapprich, A.D. Daniels, M.C. Strain, O. Farkas, D.K. Malick, A.D. Rabuck, K. Raghavachari, J.B. Foresman, J.V. Ortiz, Q. Cui, A.G. Baboul, S. Clifford, J. Cioslowski, B.B. Stefanov, G. Liu, A. Liashenko, P. Piskorz, I. Komaromi, R.L. Martin, D.J. Fox, T. Keith, M.A. Al-Laham, C.Y. Peng, A. Nanayakkara, M. Challacombe, P.M.W. Gill, B. Johnson, W. Chen, M.W. Wong, C. Gonzalez, J.A. Pople, Gaussian 03, Revision B.05, Gaussian, Inc., Pittsburgh PA, 2003.
[23] T.-S. Huang, T.J. Yale, A.R. Martin, J. Med. Chem. 12 (1969) 705–707.
[24] D. Cummins, G. Boschloo, M. Ryan, D. Corr, S.N. Rao, D. Fitzmaurice, J. Phys. Chem. B 104 (2000) 11449–11459.
[25] E.F. Godefroi, E.L. Wittle, J. Org. Chem. 21 (1956) 1163–1168.
[26] M. Harfenist, J. Org. Chem. 28 (1963) 1834–1837.
[27] C. Mackie, J. Chem. Soc. (1954) 2577–2579.
[28] R.B. Moffett, B.D. Aspergren, J. Am. Chem. Soc. 82 (1960) 1600–1607.
[29] A. Danilevicius, J. Ostrauskaite, J.V. Grazulevicius, V. Gaidelis, V. Jankauskas, Z. Tokarski, N. Jubran, J. Sidaravicius, S. Grevys, A. Dzena, J. Photochem. Photobiol. A: Chem. 163 (2004) 523–528.
[30] C.S. Kra1mer, K. Zeitler, T.J.J. Müller, Org. Lett. 2 (2000) 3723–3726.
[31] X. Hang, S. Choi, D. Choi, K. Ahn, Tetrahedron Lett. 46 (2005) 5273–5276.

[32] J.A. Vanallan, G.A. Reynolds, R.E. Adel, J. Org. Chem. 27 (1962) 1659–1664.
[33] J. Nakanishi, T. Nakajima, M. Sato, T. Ozawa, K. Tohda, Y. Umezawa, Anal. Chem. 73 (2001) 2920–2928.
[34] M. Baruah, W. Qin, C. Flors, J. Hofkens, R.A.L. Vallée, D. Beljonne, M.V.D. Auweraer, W.M.D. Borggraeve, N. Boens, J. Phys. Chem. A 110 (2006) 5998–6009.
[35] R.Y. Lai, E.F. Fabrizio, L. Lu, S.A. Jenekhe, A.J. Bard, J. Am. Chem. Soc. 123 (2001) 9112–9118.
[36] J. Dey, I.M. Warner, J. Photochem. Photobiol. A: Chem. 116 (1998) 27–37.
[37] Z. Lu, S.J. Lord, H. Wang, W.E. Moerner, R.J. Twieg, J. Org. Chem. 71 (2006) 9651–9657.
[38] B.J. Sherman, P. Bruce, A. Ambroise, K.J. Thomas, Bioconjugate Chem. 17 (2006) 387–392.
[39] J. Oshima, S. Shiobara, H. Naoumi, S. Kaneko, T. Yoshihara, A.K. Mishra, S. Tobita, J. Phys. Chem. A 110 (2006) 4629–4637.